16th World Conference on Earthquake, 16WCEE 2017

Santiago Chile, January 9th to 13th 2017

Paper N° 3903

Registration Code: S-E1461633343

NON-STATIONARY RESPONSE OF A NON-LINEAR CABLE UNDER RANDOM EXCITATION

H.T. Zhu[(1)], Y. Ding[(2)], Z.X. Li[(3)]

[(1)] Associate Professor, Key Laboratory of Coast Civil Structure Safety of Ministry of Education, Tianjin University, Tianjin 300072, China, htzhu@tju.edu.cn

[(2)] Professor, Key Laboratory of Coast Civil Structure Safety of Ministry of Education, Tianjin University, Tianjin 300072, China, dingyang@tju.edu.cn

[(3)] Professor, Key Laboratory of Coast Civil Structure Safety of Ministry of Education, Tianjin University, Tianjin 300072, China, zxli@tju.edu.cn

Abstract

A cable is a typical structural component in the field of structure engineering. Under seismic loads, the cable performs random vibration. If the excitation intensity is considerably high, the cable vibrates with a non-linear large deflection. In such a case, the quadratic and cubic non-linear terms in displacement have to be considered and the response of the cable becomes complicated. This paper presents a study on non-stationary response of a non-linear cable under random excitation by a developed path integration method. In the path integration method, the Gauss-Legendre scheme and short-time Gaussian approximation are employed to numerically obtain the probability density function (PDF) of the cable. After that, the probability density evolution process is investigated in detail. Comparison with the exact stationary solution shows that the path integration method works well for approximating the PDF solution, even in the tail region. Due to the presence of the quadratic non-linear term in displacement, the PDF solution of displacement has a non-symmetric shape, which significantly differs from a Gaussian PDF distribution. The numerical analysis further shows that the initial PDF of displacement first shifts to the positive direction along displacement in the beginning and then it turns back around the stationary PDF distribution. For different time instants, the non-stationary PDFs differ significantly from each other. At a early time instant, the peak PDF corresponding to a larger displacement is much larger than the other peaks. This indicates that in the non-stationary state, a larger displacement has a much higher probability than the prediction of the stationary case. In a dynamical reliability analysis, the critical state possibly occurs in the non-stationary process. The non-stationary PDF behavior of velocity has a similar evolution to the one of displacement .This observation should be considered in the dynamical reliability analysis of a structure.

Keywords: non-stationary response; cable; random vibration; stochastic process; probability

1. Introduction

A cable is a typical structural component in the field of structure engineering. For example, long-span cable-stayed bridges vibrate due to environmental and service loadings such as wind, rain, traffic or earthquake [1]. The use of cables in large buildings is to provide large column free area [2]. The galloping oscillations of transmission lines are self-excited motion with an extremely small excitation term [3]. The vibration of cables can be excited by direct loading on the cables or the support-induced motion, which leads to a more complicated dynamical response of a structure. Therefore, the vibration of a cable has received much attention from different aspects. Gambhir and Batchelor (1978) applied the finite element method to the study of natural frequencies and modes of vibration of sagged cables [4]. Hagedorn and Schäfer considered the effect of non-linear terms in the equations of motion on the first normal modes of the oscillations of an elastic flexible cable [3]. The Ritz-Galerkin method was used to develop the non-linear equations and to obtain approximate solutions. Luongo et al. studied planar non-linear free vibrations of an elastic cable with a deformed initial configuration [5]. The Galerkin method was also used to obtain one ordinary equation for the cable planar motion and a perturbation method was employed to derive an approximate solution. Ali investigated the forced vibrations of three dimensional sagged cables with movable supports [2]. The three non-linear coupled partial differential equations were solved using the finite difference method when the cable is excited by static and dynamical loads for fixed and movable support conditions. Later Benedettini and Rega considered the non-linear dynamical behavior of an elastic cable with the quadratic and cubic non-linearities and planar excitation [6]. They conducted a high-order perturbation analysis on the primary resonance. El-Attar et al. studied non-linear cable response to multiple support periodic excitations [7]. They first developed the coupled non-linear differential equations of cable vibration due to transverse and vertical multiple support harmonic excitations, in which the phase difference between the input support excitations at cable ends was considered. The Galerkin method was used to solve the spatial problem and the method of multiple time scales was employed to solve the temporal problem. Rega [8,9]and Ibrahim [10] made a comprehensive review on non-linear vibrations of suspended cables. The review included system modeling and methods of analysis, deterministic nonlinear phenomena arising in the finite amplitude dynamics of elastic suspended cables and the random excitation of nonlinear strings and suspended cables in air and fluid flow. In the case of random vibration, response statistics, first passage problem and power spectral density were interesting topics. Nielsen and Sichani studied stochastic and chaotic sub- and superhamonic response of shallow cables due to chord elongations [11]. The excitation was considered to be stochastically varying chord elongations caused by random vibrations of the supported structure.

As above described, the non-linear vibration of a cable has been an interesting research topic due to the occurrence of its complicated phenomena. However, the non-stationary response of a non-linear cable under random excitation is less investigated, especially for the non-stationary probability density function (PDF). As Ibrahim reviewed [10], when a cable is under random excitation, response statistics, first passage problem and power spectral density have to be obtained. These concerned variables mostly rely on the PDFs of response. This motivates the authors to carry out a study for the non-stationary PDF of a non-linear cable under random excitation. In this paper, a path integration analysis is conducted on the non-stationary PDF of a non-linear cable under random excitation. This paper considers the non-linear dynamical behavior of an elastic cable with the quadratic and cubic non-linearities and planar excitation. As the adopted path integration method is concerned, the interpolation scheme is based on the Gauss-Legendre quadrature integration rule [12] and the short-time transition probability density is based on short-time Gaussian approximation [13,14]. The present work extends the path integration method to the case of non-linear random vibration of a cable. After that, the probability density evolution process is investigated in detail. Comparison with the exact stationary solution shows that the path integration method works well for approximating the PDF solution, even in the tail region. Due to the presence of the quadratic non-linear term in displacement, the PDF solution of displacement has a non-symmetric shape, which significantly differs from a Gaussian PDF distribution. This difference should be considered in reliability analysis.

2. Problem formulation

For the sake of simplicity, the non-linear random vibration of a cable can be mathematically expressed in a non-dimensional form [6,15]

$$\ddot{u} + c\dot{u} + k_1 u + k_2 u^2 + k_3 u^3 = \xi(t) \tag{1}$$

where u is the first-mode amplitude; c is the damping coefficient; k_1, k_2 and k_3 are the stiffness parameters. $\xi(t)$ is the Gaussian white noise and its statistics are as follows

$$\mathrm{E}[\xi(t)] = 0,\ \mathrm{E}[\xi(t)\xi(t+\tau)] = 2\pi K\delta(\tau) \tag{2}$$

where $2\pi K$ is the excitation intensity and $\delta(\tau)$ is the Dirac delta function. Let $u = x$ and $\dot{u} = y$, Eq. (1) can be reformulated in a set of first-order differential equations

$$\begin{cases} \dot{x} = y \\ \dot{y} = -cy - k_1 x - k_2 x^2 - k_3 x^3 + \xi(t) \end{cases} \tag{3}$$

According to Eq. (3), the associated Fokker-Planck-Kolmogorov (FPK) equation is established below

$$\frac{\partial q}{\partial t} = -y\frac{\partial q}{\partial x} + \frac{\partial}{\partial y}[(cy + k_1 x + k_2 x^2 + k_3 x^3)q] + \pi K\frac{\partial^2 q}{\partial y^2} \tag{4}$$

where $q = q(x, y, t \,|\, x^{(0)}, y^{(0)}, t_0)$ is the joint PDF of the response of the non-linear cable. The FPK equation is to be solved under the initial condition

$$q(x, y, t \,|\, x^{(0)}, y^{(0)}, t_0) = \delta(x - x^{(0)})\delta(y - y^{(0)}) \tag{5}$$

and some specified boundary conditions.

Due to the complicated form of Eq. (4), the exact non-stationary PDF solution is hardly obtained. If the stationary PDF is considered and the term on the left-hand side equals to zero, the stationary FPK equation can be solved exactly. The stationary PDF is given below

$$q(x, y) = C\exp\left\{-\frac{c}{2\pi K}[y^2 + k_1 x^2 + \frac{2}{3}k_2 x^3 + \frac{1}{2}k_3 x^4]\right\} \tag{6}$$

where C is the normalized constant. Eq. (6) presents a stationary PDF because the PDF is independent of time t and the initial condition.

In order to obtain the non-stationary PDF solution, the path integration method is adopted. The solution procedure of the adopted path integration method is given as follows.

First assuming that $\mathbf{x}(t)$ is a vector containing n entries, the PDF of $\mathbf{x}(t)$ at $t = t_{i-1}$ is given below

$$p(\mathbf{x}^{(i)}, t_i) = \int_{R_s} q(\mathbf{x}^{(i)}, t_i \,|\, \mathbf{x}^{(i-1)}, t_{i-1})\, p(\mathbf{x}^{(i-1)}, t_{i-1})\, d\mathbf{x}^{(i-1)} \tag{7}$$

where $p(\mathbf{x}^{(i-1)}, t_{i-1})$ is the PDF of $\mathbf{x}(t)$ when $t = t_{i-1}$. $p(\mathbf{x}^{(0)}, t_0)$ is the PDF of $\mathbf{x}(t)$ at the initial time $t = t_0$. $q(\mathbf{x}^{(i)}, t_i \,|\, \mathbf{x}^{(i-1)}, t_{i-1})$ is the transition probability density which is determined by the FPK equation. R_s is the reduced n-dimensional space of $\mathbf{x}(t)$. The PDF of $\mathbf{x}(t)$ can be reformulated below

$$\begin{aligned} p(\mathbf{x}, t) = &\int_{R_s} q(\mathbf{x}, t \,|\, \mathbf{x}^{(N-1)}, t_{N-1})\, p(\mathbf{x}^{(N-1)}, t_{N-1})\, d\mathbf{x}^{(N-1)} \\ &\times \int_{R_s} q(\mathbf{x}^{(N-1)}, t_{N-1} \,|\, \mathbf{x}^{(N-2)}, t_{N-2})\, p(\mathbf{x}^{(N-2)}, t_{N-2})\, d\mathbf{x}^{(N-2)} \\ &\times \cdots \int_{R_s} q(\mathbf{x}^{(2)}, t_2 \,|\, \mathbf{x}^{(1)}, t_1)\, p(\mathbf{x}^{(1)}, t_1)\, d\mathbf{x}^{(1)} \times \int_{R_s} q(\mathbf{x}^{(1)}, t_1 \,|\, \mathbf{x}^{(0)}, t_0)\, p(\mathbf{x}^{(0)}, t_0)\, d\mathbf{x}^{(0)} \end{aligned} \tag{8}$$

This means that the path integration method discretize Eq. (8) at a finite number of state integral points of space and time. The values of $q(\mathbf{x}^{(i)}, t_i \mid \mathbf{x}^{(i-1)}, t_{i-1})$ and $p(\mathbf{x}^{(i-1)}, t_{i-1})$ can be approximated by the corresponding grid points. The stepwise evaluation of the PDF can be implemented using the splines interpolation method [16] or the Gauss-Legendre integration scheme [12]. In this paper, the Gauss-Legendre integration scheme is used and the expression of two-dimensional integration is given below

$$p(x_r^i, y_s^i, t_i) = \frac{\Delta_x}{2}\frac{\Delta_y}{2}\sum_{k=1}^{2n}\sum_{l=1}^{2m} p(x_k^{(i-1)}, y_l^{(i-1)}, t_{i-1}) q(x_r^i, y_s^i, t_i \mid x_k^{(i-1)}, y_l^{(i-1)}, t_{i-1}) \tag{9}$$

where n and m are the interval numbers along x-direction and y-direction; Δ_x and Δ_y are the lengths of sub-intervals along x-direction and y-direction; x_r and y_s are the Gaussian quadrature points.

For the k th interval along x-direction

$$\begin{cases} x_i = x_L + 0.2113(x_R - x_L) \\ x_{i+1} = x_R - 0.2113(x_R - x_L) \end{cases} \tag{10}$$

where $i = (k-1)\times 2 + 1$ and $k = 1,\ldots,n$. x_L is the left boundary of the k th interval and x_R is the right boundary of the k th interval.

For the l th interval along y-direction

$$\begin{cases} y_j = y_L + 0.2113(y_R - y_L) \\ y_{j+1} = y_R - 0.2113(y_R - y_L) \end{cases} \tag{11}$$

where $j = (l-1)\times 2 + 1$ and $l = 1,\ldots,m$. y_L is the left boundary of the l th interval and y_R is the right boundary of the l th interval.

$p(x_k^{(i-1)}, y_l^{(i-1)}, t_{i-1})$ is the PDF of the Gaussian quadrature point (x_k , y_l) at the time instant $t = t_{i-1}$. According to the probability theory, the PDFs of the Gaussian quadrature points at $t = t_i$ can be accessible given that the PDFs of the Gaussian quadrature points and their transition PDFs are known at $t = t_{i\text{-}1}$.

When the time increment is small, the Gaussian assumption of the transition probability density is acceptable [14]. Sun and Hsu proposed a short-time Gaussian approximation for the transition probability density through the Gaussian closure method. This approximation for the transition probability density is employed in this paper and the transition probability density is given below

$$\begin{aligned} q(x_r^{(i)}, y_s^{(i)}, t_i \mid x_k^{(i-1)}, y_l^{(i-1)}, t_{i-1}) &= \frac{1}{2\pi\sigma_{x_k^{(i-1)}}\sigma_{y_l^{(i-1)}}\sqrt{1-\rho^2_{x_k^{(i-1)}y_l^{(i-1)}}}} \\ &\times \exp\left\{-\frac{1}{2(1-\rho^2_{x_k^{(i-1)}y_l^{(i-1)}})}\left(\left(\frac{x_r^{(i)} - m_{x_k^{(i-1)}}}{\sigma_{x_k^{(i-1)}}}\right)^2\right.\right. \\ &\left.\left. - 2\rho_{x_k^{(i-1)}y_l^{(i-1)}}\left(\frac{x_r^{(i)} - m_{x_k^{(i-1)}}}{\sigma_{x_k^{(i-1)}}}\right)\left(\frac{y_s^{(i)} - m_{y_l^{(i-1)}}}{\sigma_{y_l^{(i-1)}}}\right) + \left(\frac{y_s^{(i)} - m_{y_l^{(i-1)}}}{\sigma_{y_l^{(i-1)}}}\right)^2\right)\right\} \end{aligned} \tag{12}$$

where $m_{x_k^{(i-1)}}$ and $m_{y_l^{(i-1)}}$ are the means of x_k^{i-1} and y_l^{i-1}, respectively. $\rho_{x_k^{(i-1)}y_l^{(i-1)}}$ is the correlation coefficient of x_k^{i-1} and y_l^{i-1}.

Eq. (13) can be formulated using the results of the Gaussian closure method. According to Eq. (13), the corresponding moment equations can be established

$$\begin{cases} \dot{m}_{10} = m_{01} \\ \dot{m}_{01} = -k_3 m_{30} - k_2 m_{20} - k_1 m_{10} - c m_{01} \\ \dot{m}_{20} = 2m_{11} \\ \dot{m}_{11} = -k_3 m_{40} - k_2 m_{30} - k_1 m_{20} - c m_{11} + m_{02} \\ \dot{m}_{02} = -2k_3 m_{31} - 2k_2 m_{21} - 2k_1 m_{11} - 2c m_{02} + 2\pi K \end{cases} \tag{13}$$

where $m_{rs} = E[x^r y^s]$. In Eq. (13), some higher-order moment terms exist, which means that the set of equations are not closed themselves. Therefore, the Gaussian closure method is adopted to make the higher-order moment terms be expressed by the first-order and second-order moment terms. These expressions are given below:

$$\begin{cases} m_{30} = 3m_{10} m_{20} - 2m_{10}^3 \\ m_{21} = -2m_{01} m_{10}^2 + 2m_{11} m_{10} + m_{01} m_{20} \\ m_{40} = 3m_{20}^2 - 2\mathrm{m}_{10}^4 \\ m_{31} = 3m_{11} m_{20} - 2m_{01} m_{10}^3 \end{cases} \tag{14}$$

Eqs. (13) and (14) are simultaneously solved by the fourth-order Runge-Kutta algorithm. The initial solution at the time instant t_i is given as

$$\boldsymbol{m}^{(0)} = \left[m_{10}^{(0)}, m_{01}^{(0)}, m_{20}^{(0)}, m_{11}^{(0)}, m_{02}^{(0)}\right] = \left[x_k^{(i-1)}, y_l^{(i-1)}, \left(x_k^{(i-1)}\right)^2, x_k^{(i-1)} y_l^{(i-1)}, \left(y_l^{(i-1)}\right)^2\right] \tag{15}$$

After that, the first-order and second-order moments can be obtained with respect to time. The transition PDF has a significant value only in the neighborhood of the starting point $\left(x_k^{(i-1)}, y_l^{(i-1)}\right)$. Only a few destination Gaussian points are needed in Eq. (9). The computational at other points can be eliminated, which significantly reduces the computational efforts. The detail can be referred to Ref. [17].

3. Illustrative example

In order to show the effectiveness of the path integration method, an example is further studied. The parameters of Eq. (1) and Eq. (2) are defined as follows: $c = 0.1$; $k_1 = 1.0$, $k_2 = 1.0$, $k_3 = 0.3$ and $2\pi K = 0.2$. The initial condition is given below

$$p(x^{(0)}, y^{(0)}) = \frac{1}{2\pi s_1 s_2} \exp\left\{-\frac{(x^{(0)} - \mu_1)^2}{2s_1^2} - \frac{(y^{(0)} - \mu_2)^2}{2s_2^2}\right\} \tag{16}$$

where $\mu_1 = -1.5$, $\mu_2 = -2.0$, $s_1 = 0.1$ and $s_2 = 0.1$.

In the path integration method, the state space is $[-6, 6] \times [-6, 6]$, which is divided into 60 uniform sub-intervals along each direction with two quadrature points in each sub-interval. The time step is taken as 1.0 for formulating the transition PDF solution with the short-time Gaussian approximation. In the numerical analysis, the non-stationary PDF and stationary PDF of the non-linear cable are both studied.

The exact stationary PDF solution is obtained using the expression of Eq. (6). The state space of x and y is the same as the one used in the path integration method, i.e., $[-6, 6] \times [-6, 6]$. The Gauss-Legendre quadrature integration rule is also used to obtain the values of the exact stationary PDF at each Gaussian quadrature point. In Eq. (6), the normalized constant C can be determined considering the fact that the probability is unit by integrating the PDF over the entire state space as Eq. (17) shows

$$\int_{R_s} q(x, y) dx \mathrm{d}y = 1 \tag{17}$$

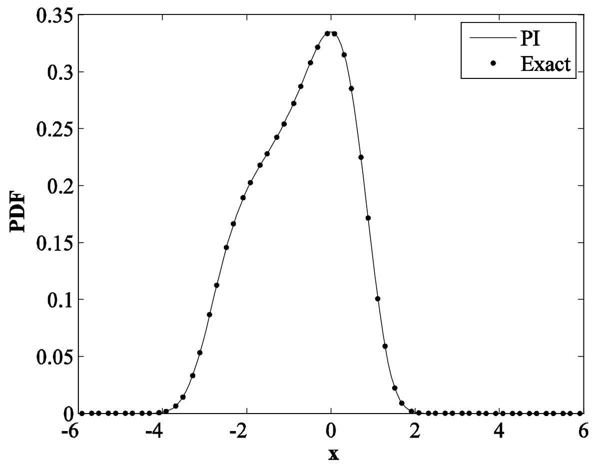

(a) PDF of displacement

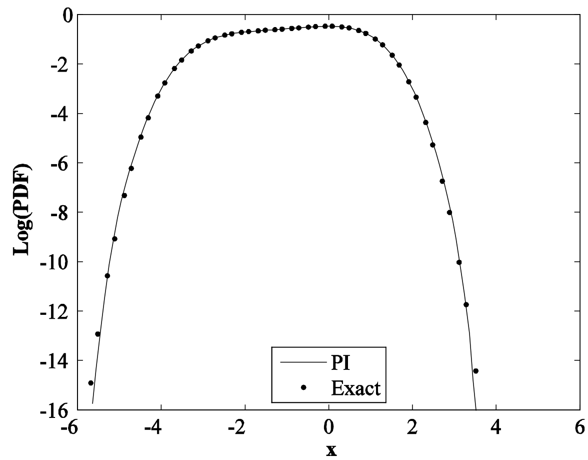

(b) Logarithmic PDF of displacement

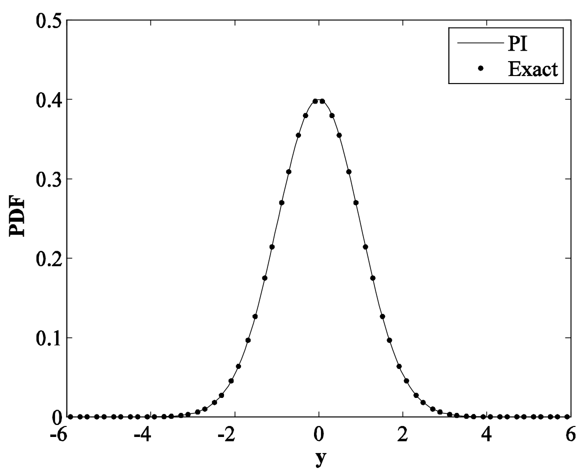

(c) PDF of velocity

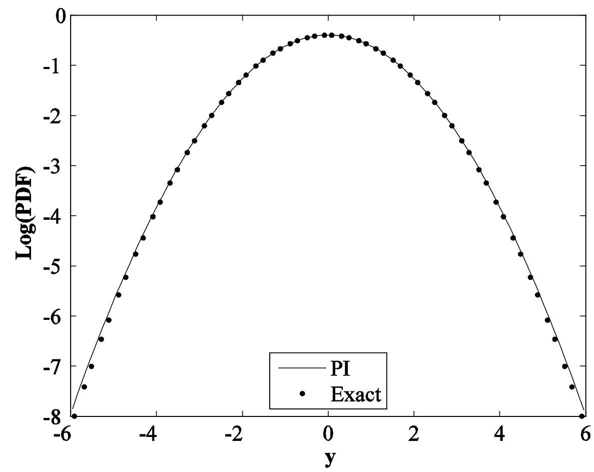

(d) Logarithmic PDF of velocity

Fig. 1 Comparison between the path integration method (PI) and the exact solution (Exact)

In the numerical analysis, the time duration $t = 100$ is taken as the stationary PDF solution of the path integration method. The longer duration cannot significantly improve the accuracy of the result but it takes much more computational times. Fig. 1 presents the comparison on the results obtained with the path integration method with the exact solution. Fig. 1(a) shows that the displacement has a non-symmetric PDF distribution and the path integration method provides a satisfactory PDF solution compared with the exact solution. This agreement can be observed in the tail region as shown in Fig. 1(b). The good agreement can be made even at the probability level of 1×10^{-16}. Fig. 1(b) also shows that the PDF distribution of displacement has a non-symmetric shape and the mean is non-zero.

The quadratic term in the restoring force in Eq. (1) results in the cubic-order term of displacement in the exponential of PDF in Eq. (6). The cubic term of displacement in Eq. (6) causes the non-zero mean and a non-symmetric PDF distribution of displacement. When a failure probability is concerned in the tail region for the system in Eq. (1), the failure probabilities of the left and right ranges of displacement are significantly different, which should be paid attention to in the reliability design of such a kind of system. Consequently, the conventional assumption on a symmetric PDF distribution is no longer valid in reliability analysis. This is a difference of cable vibration from other member vibrations. As expected, if the magnitude of the cubic term in Eq. (6) increases, the non-symmetric PDF distribution of displacement will be more significant. Therefore, the effects of the quadratic term in the restoring force in Eq. (1) are worth investigating widely.

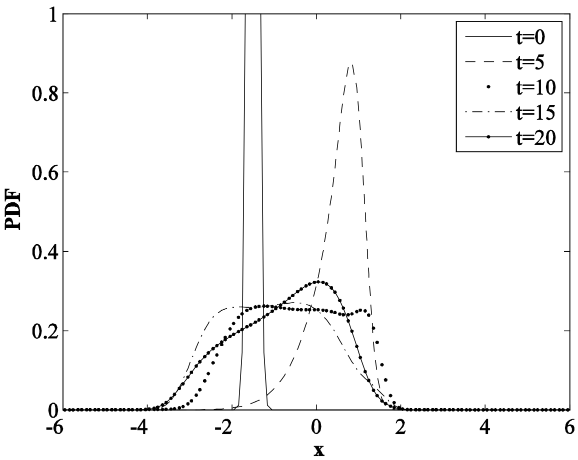

(a) Non-stationary PDFs of displacement

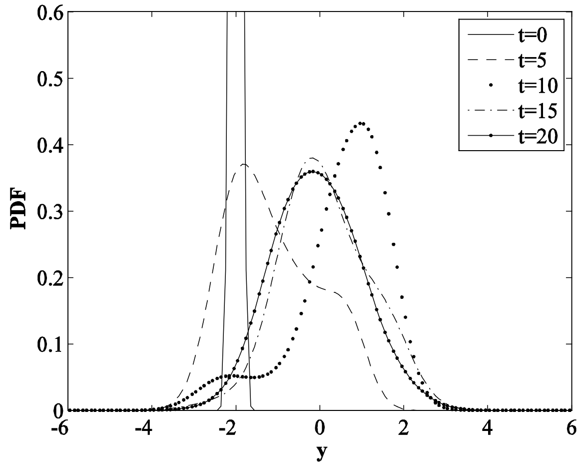

(b) Non-stationary PDFs of velocity

Fig. 2 Comparison on the PDF evolution of the non-linear cable from $t = 0$ to $t = 20$

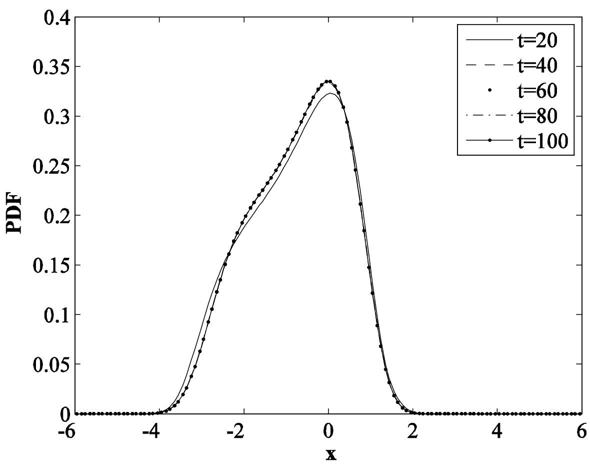

(a) Non-stationary PDFs of displacement

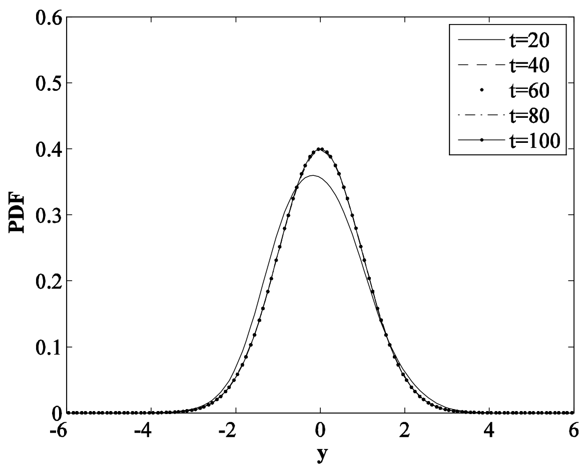

(b) Non-stationary PDFs of velocity

Fig. 3 Comparison on the PDF evolution of the non-linear cable from $t = 20$ to $t = 100$

As the case of velocity is concerned, Fig. 1(c) and 1(d) provide a comparison on the results obtained with the path integration method with the exact solution for velocity. The good agreement is also made between the path integration method with the exact solution, even in the tail region. By contrast, the PDF distribution of velocity has a symmetric shape and its mean is zero. As shown in Fig. 1(c), the good agreement can be made even at the probability level of 1×10^{-8}. The different behavior between displacement and velocity can be explained using the expression of Eq. (6). For the exact stationary PDF solution, Eq. (6) has no cross term between displacement and velocity, which means that displacement and velocity is not correlated to each other in stationary state. Therefore, the PDFs of displacement and velocity present different PDF distributions.

Next, the PDF evolution of the non-linear cable is studied in detail from the beginning to the stationary statement. Fig. 2 presents the PDF evolution of the non-linear cable from $t = 0$ to $t = 20$ while Fig. 3 compares the PDF evolution of the non-linear cable from $t = 20$ to $t = 100$. As shown in Fig. 2, the non-stationary PDF of the response significantly varies. Because the initial condition Eq. (16) has a much higher peak than other non-stationary PDFs, Fig. 2 do not show the whole distribution of the initial PDF in order to make the PDF evolution at other time instant clear. Fig. 2 shows that the initial PDF of displacement first shifts to the positive direction along displacement until $t = 5$ and then it turns back around the stationary PDF distribution. For different time instants, the non-stationary PDFs differ significantly from each. At the time instant $t = 5$, the peak PDF corresponding to a larger displacement is much larger than the one of $t = 20$. This indicates that in the non-stationary state, a larger displacement has a much higher probability than the prediction of the stationary case. In a dynamical reliability analysis, the critical state possibly occurs in the non-stationary process. In the case of velocity, the similar observations can be made.

When the time duration is from $t = 20$ to $t = 100$ as shown in Fig. 3, the PDF evolves nearly to the stationary state. Fig. 3 indicates that there is no significant difference from $t = 40$ to $t = 100$ indicating that the cable reaches a stationary state about at $t = 40$.

4. Conclusions

The random vibration of a non-linear cable is considered in this paper. The equation of motion of the cable is formulated about the first-mode amplitude in a non-dimensional form. In this equation, the quadratic and cubic non-linear terms in displacement are considered. The non-stationary PDF of the cable is solved by a developed path integration method. In the path integration method, the Gauss-Legendre scheme and short-time Gaussian approximation are employed to numerically obtain the probability density function (PDF) of the cable. After that, the probability density evolution process is investigated in detail. Comparison with the exact stationary solution shows that the path integration method works well for approximating the PDF solution, even in the tail region. Due to the presence of the quadratic non-linear term in displacement, the PDF solution of displacement has a non-symmetric shape, which significantly differs from a Gaussian PDF distribution. The numerical analysis further shows that the initial PDF of displacement first shifts to the positive direction along displacement in the beginning and then it turns back around the stationary PDF distribution. For different time instants, the non-stationary PDFs differ significantly from each other. At a early time instant, the peak PDF corresponding to a larger displacement is much larger than the other peaks. This indicates that in the non-stationary state, a larger displacement has a much higher probability than the prediction of the stationary case. In a dynamical reliability analysis, the critical state possibly occurs in the non-stationary process. The non-stationary PDF behavior of velocity has a similar evolution to the one of displacement .This observation should be considered in the dynamical reliability analysis of a structure.

5. Acknowledgements

This research was jointly supported by the National Natural Science Foundation of China under Grant No. 51478311, the Natural Science Foundation of Tianjin, China under Grant No. 14JCQNJC07400, and the Innovation Foundation of Tianjin University under Grant No. 0903061014.

6. References

[1] Xia Y, Fujino Y (2006): Auto-parametric vibration of a cable-stayed-beam structure under random excitation. *Journal of Engineering Mechanics*, **132**(3), 279-286.

[2] Ali SA (1986): Dynamic response of sagged cables. *Computers & Structures*, **23**(1), 51-57, 1986.

[3] Hagedorn P, Schäfer B (1980): On non-linear free vibrations of an elastic cable, International Journal of Non-Linear Mechanics, **15**(4-5), 333-340.

[4] Gambhir ML, Batchelor BD (1978): Parametric study of free vibration of sagged cables, *Computers & Structures*, **8**, 641-648.

[5] Luongo A, Rega G, Vestroni F (1984): Planar non-linear free vibrations of an elastic cable. *International Journal of Non-Linear Mechanics*, **19**(1), 39-52.

[6] Benedettini F, Rega G (1987): Non-linear dynamics of an elastic cable under planar excitation. *International Journal of Non-Linear Mechanics*, **22**(6), 497-509.

[7] El-Attar M, Ghoharah A, Aziz TS (2000): Non-linear cable response to multiple support periodic excitation. *Engineering Structures*, **22**(10), 1301-1312.

[8] Rega G (2004): Nonlinear vibrations of suspended cables-part I: modeling and analysis. *Applied Mechanics Review*, **57**(6), 443-478.

[9] Rega G (2004): Nonlinear vibrations of suspended cables-part II: deterministic phenomena. *Applied Mechanics Review*, **57**(6), 479-514.

[10] Ibrahim RA (2004): Nonlinear vibrations of suspended cables-part III: random excitation and interaction with fluid flow. *Applied Mechanics Review*, **57**(6), 515-549.

[11] Nielsen SRK, Sichani MT (2011): Stochastic and chaotic sub- and superharmonic response of shallow cables due to chord elongations. *Probabilistic Engineering Mechanics*, **26**(1), 44-53.

[12] Yu JS, Cai GQ, Lin YK (1997): A new path integration procedure based on Gauss-Legendre scheme. *International Journal of Non-Linear Mechanics*, **32**(4), 759-768.

[13] Sun JQ, Hsu CS (1988): First-passage time probability of non-linear stochastic systems by generalized cell mapping method. *Journal of Sound and Vibration*, **124**(2), 233-248.

[14] Sun JQ, Hsu CS (1990): The generalized cell mapping method in nonlinear random vibration based upon short-time Gaussian approximation. Journal of Applied Mechanics, **57**(4), 1018-1025.

[15] Kovacic I, Brennan MJ (2011): *The Duffing Equation: Nonlinear Oscillators and their Behaviour*, John Wiley and Sons, Ltd., Publication.

[16] Naess A, Moe V (2000): Efficient path integration methods for nonlinear dynamic systems. *Probabilistic Engineering Mechanics*, **15**(2), 221–231.

[17] Zhu HT, Duan LL (2016): Probabilistic solution of non-linear random ship roll motion by path integration. *International Journal of Non-Linear Mechanics*, **83**, 1-8.